TECHNICAL MEMORANDUM

531

Detection of extreme events from a SAR image spectrum

Peter A.E.M. Janssen

Research Department

July 27, 2007

European Centre for Medium-Range Weather Forecasts
Europäisches Zentrum für mittelfristige Wettervorhersage
Centre européen pour les prévisions météorologiques à moyen terme

Series: ECMWF Technical Memoranda

A full list of ECMWF Publications can be found on our web site under:
http://www.ecmwf.int/publications/

Contact: library@ecmwf.int

Abstract

It is shown that the nonlinear mapping relation between a surface gravity wave spectrum and its SAR image spectrum, as derived by Hasselmann and Hasselmann (1991), is not complete. The reason for this is that the velocity bunching effect is so nonlinear that effects of skewness are as important as the nonlinear terms already retained in the Hasselmann and Hasselmann approach. Furthermore, certain effects of kurtosis need to be retained as well, but these will mainly affect the shape of the azimuthal correlation function. For a Gaussian sea the azimuthal correlation function, which reflects the statistical properties of the sea surface, can be approximated by a Gaussian function, This is expected to be an adequate model in most cases. However, for extreme waves there are departures from the Normal distribution. This then will result in departures from the Normal shape of the azimuthal correlation function as well. In other words, an analysis of the azimuthal cutoff may reveal information on the non-gaussian statistics of the sea surface, and may indicate the enhanced occurrence of freak waves.

1 Introduction

Nowadays there is an increased understanding of the reasons why freak waves may occur. On the open ocean there are at least three mechanism responsible for the formation of freak waves. The first one is linear superposition of waves. In this case the surface elevation probability distribution is a Gaussian giving relatively small probabilities that extreme sea states may occur. A more promising mechanism is nonlinear focussing of a unimodal wave system, because in such a case there may be, as reflected by finite values of the kurtosis, considerable deviations from the Normal distribution resulting in an increased probability of extreme events. Thirdly, nonlinear focussing may play an even more pronounced role in crossing sea states. An otherwise stable windsea system may become unstable in the presence of a second, swell system.

Freak waves have been simulated numerically (in 1D and even in 2 D) and have been generated in the laboratory. Inspecting time series from buoys it is found that extreme sea states really occur (and perhaps more frequently then previously thought). In order to improve on safety of shipping, it is of the utmost importance to be able to predict the occurrence of freak waves. Modern wave forecasting systems determine the evolution of the wave spectrum, but do not provide information on the phases of the waves. Hence, it is not possible to predict individual wave events. However, recently (Janssen, 2003) it was realized that the nonlinear four-wave interactions imply a relation between spectral shape and the deviation of the surface elevation probability distribution function (pdf) from the normal gaussian distribution. Here large deviations with positive kurtosis correspond to the likely occurrence of freak waves. In one dimension, this theory has been succesfully validated against laboratory observations from the big wave tank in Trondheim. This suggests that we can predict the probability that extreme, freak waves do occur (probablistic wave forecasting). As a consequence, at ECMWF a freak wave warning system has been implemented in October 2003.

Clearly, it is highly desirable to validate present ideas on freak wave formation on a global scale. In particular it is important to try to validate the expected relation between the occurrence of extreme events and the statistical properties of the sea surface, i.e. the shape of the pdf. Also, is it indeed so that there is a relation between spectral shape and deviations from Normality? This requires that one needs to be able to monitor the statistical distribution of the surface elevation and the wave spectrum at the same time. Although in theory a radar altimeter could provide statistical information (Lipa and Barrick, 1981) as the waveform is a reflection of the pdf of the sea surface, it does not measure the wave spectrum. For this reason we follow an alternative approach and we ask ourselves the question whether a Synthetic Aperture Radar could provide, in addition to wave spectra, information on the statistical properties of the sea surface.

The plan of this paper is as follows. First, a brief review of the SAR measurement theory is given. A SAR basically measures the modulation of the short ocean wave spectrum by the long ocean waves, and other oceanographic and atmospheric phenomena. For low to moderate sea states those modulations are caused by tilt and hydrodynamic motion of the backscattering elements (facets) by the long waves. For the SAR there is also a modulation due to 'velocity bunching' which is related to locating the position of the facet in the azimuth (flight) direction at zero Doppler shift. This determines in principle the SAR image, which is basically the spatial distribution of intensity of the radar backscatter. In order to obtain a relation with the ocean wave spectrum Hasselmann and Hasselmann (1991) (denoted by H&H from now onwards) make use of the statistical property of ocean waves that the pdf of the sea surface elevation is approximately a Gaussian distribution. For such a distribution it is indeed possible to establish a relation between the SAR image spectrum and the surface gravity wave spectrum, provided the tilt and hydrodynamic modulation and velocity bunching are linearly related to the surface elevation. Here, we present a generalization of the result of H&H using the Gram-Charlier distribution, which describes deviations of Normality in terms of cumulants of the distribution. Following the approach of Krogstad (1992) it is then possible to obtain a general expression for the SAR image spectrum in terms of the cumulants of the modulation in the intensity and the azimuthal displacement. For weakly nonlinear waves it is possible to estimate all the relevant cumulants, and it turns out that a number of contributions related to the third and fourth cumulant are as important as the nonlinear term of the H&H nonlinear mapping relation (1991). The reason that these cumulants are important is explained by pointing out that for SARs flying on board of polar orbiting platforms the velocity bunching mechanism is very nonlinear. Thus, the H&H nonlinear mapping is not complete. However, it can be shown that only effects of the third (skewness) and fourth (kurtosis) cumulant need to be included in order to get a complete description. Finally, in order obtain a closed nonlinear mapping relation for the SAR image the cumulants need to be evaluated in terms of the wave spectrum which is a second order cumulant (or moment). For weakly nonlinear waves it is shown how this is possible for both the third and the fourth moment, but approximate solutions of the dynamical equations for surface gravity waves are required.

2 SAR measurement theory

In this section a brief description is given of our present knowledge of the SAR imaging mechanism. Expressions for modulations in the SAR image caused by tilt and the local advection velocity of the long waves, and caused by velocity bunching are known for small amplitude waves. Next, we start from a general intensity field and a general azimuthal displacement field with known statistical properties and we derive the general relation between the SAR image spectrum and the cumulants of the intensity field and the azimuthal displacement field.

A brief overview of the SAR measurement theory is now given (taken from Section V.3 and V.4 of Komen *et al.*, 1994). A SAR is capable of detecting a variety of larger scale, oceanic phenomena which modulate the short (Bragg) ocean ripple spectrum, such as fronts, internal waves, natural surface films, bottom topography and ocean gravity waves. Of particular interest has always been the SAR imaging of ocean waves. The modulation of the short waves by the longer ocean waves may be described by a two-scale model as the long waves have scales that are much larger than the wavelength of the backscattering ripple waves. According to Bragg theory, the return signal from the individual backscattering facets of the ocean surface arises through a resonant interaction with the two Bragg components propagating towards and away from the antenna. In the two-scale model the facet is regarded as large compared to the Bragg wave and small compared the the long waves of interest. The orientation and local velocity of the facet are determined by the local slope and orbital velocity of the long waves. Bragg theory is then applied to the local facet in a coordinate system with respect to the facet normal and moving with the local advection velocity of the facet.

Modulations of the Radar backscatter now arise through a) variation in the local angle of incidence associate with variations in the facet normal (*tilt modulation*, cf. Alpers and Hasselmann, 1978) and b) variations in the energy of the Bragg backscattering ripples caused by hydrodynamic interactions between the short ripples and

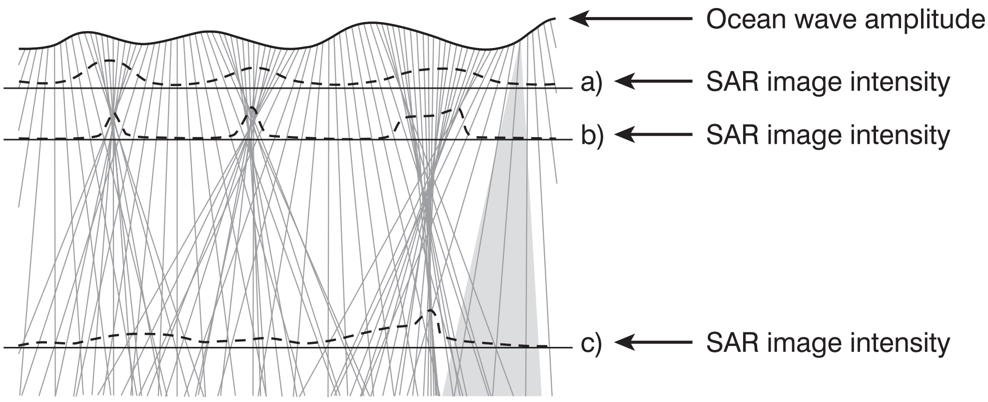

Figure 1: Azimuthal displacement of a facet in the SAR image plane due to the long wave orbital velocity. a) Linear Imaging; b,c) Strongly nonlinear Imaging.

the longer waves (*hydrodynamic modulation*, cf. Wright, 1968; Feindt *et al.*, 1986).

The superposition of the tilt and hydrodynamic modulation transfer function (MTF) yields the RAR (real aperture radar) MTF. In addition to these two mechanisms, there exists for the SAR an important third modulation mechanism, which is termed *velocity bunching*. This is related to the use of phase information by the SAR to locate the azimuthal position of a facet: a facet is positioned at the azimuthal location of zero Doppler shift. The advection of the local facet by the long waves induces an additional Doppler shift which is misinterpreted by the SAR as an azimuthal offset of the position of the facet. This is accompanied by variations in the apparent facet density in the SAR image, which enables waves to be seen even when no Radar cross-section modulation is present. The azimuthal displacement ξ (see Appendix) is found to be proportional to the product of the range component of the orbital velocity of the waves and $\beta = R/V$ which is the range R to velocity V ratio of the SAR platform. When the displacement is small compared to the length of the wave of interest, the velocity bunching effect is linear. However, if the facet displacement becomes comparable or larger than the length of the longer waves, the wave patterns in the SAR image become severely distorted and can even be completely smeared out. This ultimately limits the azimuthal resolution of the SAR at a finite cutoff wavenumber. This is illustrated in Fig. 1 for increasing nonlinearity of the ocean waves. In particular, for polar orbiting platforms with large values of $\beta = \mathscr{O}(100)$ s, the velocity bunching effect is a serious issue.

The velocity bunching mechanism is a purely geometrical, fully determined process. If the RAR MTF is also known, the mapping of the sea surface into the SAR image plane and the nonlinear transformation of the wave spectrum into the SAR image spectrum can be computed for a given realization of the sea surface. This is the basis of the Monte Carlo approach of Brüning *et al.* (1988) where for a given spectrum a number of random realizations of an instantaneous ocean-wave field is created. For each member of the ensemble the sea surface is mapped into the SAR image plane. Fourier transformation of the image and averaging of the squared amplitudes then gives an estimate of the SAR image variance spectrum.

A second approach, which we will study in more detail below, takes advantage of the known statistical properties of the sea surface. For a Gaussian sea state, Hasselmann and Hasselmann (1991) (see also Krogstad, 1992) were able to express all higher order nonlinear properties of the wave field in terms of the wave spectrum and to derive a closed integral transform relation between the wave spectrum and the SAR image spectrum. Here, we will redo this derivation, but now for a more general statistical distribution.

In summary, in the framework of linear modulation theory the surface elevation $\eta(\mathbf{x},t)$ and the local backscatter cross section $\sigma(\mathbf{x},t)$ are represented by a superposition of surface gravity waves. From the outset we adopt a continuous representation, hence

$$\eta(\mathbf{x},t) = \int_{-\infty}^{\infty} d\mathbf{k}\, \hat{\eta}(\mathbf{k}) \exp(i\theta) + \text{c.c}$$
$$\sigma(\mathbf{x},t) = \bar{\sigma}\left[1 + \int_{-\infty}^{\infty} d\mathbf{k}\, \hat{\sigma}(\mathbf{k}) \exp(i\theta) + \text{c.c}\right] \tag{1}$$

where $\theta = \mathbf{k}.\mathbf{x} - \omega t$, $\omega = (gk)^{1/2}$ denotes the dispersion relation and $\bar{\sigma}$ denotes the spatially averaged cross section. The cross section modulation amplitude $\hat{\sigma}$ and the wave amplitude $\hat{\eta}$ are linearly related through the RAR modulation transfer function $T_R(\mathbf{k})$,

$$\hat{\sigma}(\mathbf{k}) = T_R(\mathbf{k})\hat{\eta}(\mathbf{k}). \tag{2}$$

Here, $T_R(\mathbf{k})$ may be decomposed into its tilt and hydrodynamic contributions,

$$T_R(\mathbf{k}) = T_T(\mathbf{k}) + T_H(\mathbf{k}), \tag{3}$$

but for present purposes we do not need to further specify the modulation transfer function. The resulting RAR image will be denoted by $I_R(\mathbf{x})$ and it is directly proportional to the backscatter cross section σ at a certain instant in time, say $t = 0$. Hence,

$$I_R(\mathbf{x}) = \sigma(\mathbf{x}, 0) \tag{4}$$

Introduce the Fourier decomposition of $I_R(\mathbf{x})$,

$$I_R(\mathbf{x}) = \int_{-\infty}^{\infty} d\mathbf{k}\, \hat{I}_R(\mathbf{k}) \exp(i\mathbf{k}.\mathbf{x}), \tag{5}$$

where because of reality of the image intensity $\hat{I}_R(\mathbf{k}) = \hat{I}_R^*(-\mathbf{k})$. Then, using Eqns. (5), (1) and (2), $\hat{I}_R(\mathbf{k})$ can be expressed as

$$\hat{I}_R(\mathbf{k}) = T_R(\mathbf{k})\eta(\mathbf{k}) + (T_R(-\mathbf{k})\eta(-\mathbf{k}))^* \tag{6}$$

showing that the RAR image is indeed a frozen image of the surface.

The SAR image suffers, however, considerable modifications from the frozen image due to motion effects. Here, only the so-called velocity bunching effect is considered which gives rise to an azimuthal displacement of the apparent position of a facet in the image plane. In the Appendix a derivation of this azimuthal offset is presented. The azimuthal displacement $\xi(\mathbf{x})$ at a location $\mathbf{x}$ is then given by

$$\xi(\mathbf{x}) = \beta v \tag{7}$$

where v is the range component of the orbital velocity of the waves. In linear approximation the velocity v is related to the surface elevation amplitude according to

$$v = \int_{-\infty}^{\infty} d\mathbf{k}\, T_V(\mathbf{k})\hat{\eta}(\mathbf{k}) \exp(i\mathbf{k}.\mathbf{x}) + \text{c.c}, \tag{8}$$

where

$$T_V(\mathbf{k}) = -\omega\left(\sin\theta \frac{k_r}{|k|} + i\cos\theta\right) \tag{9}$$

with θ the radar incidence angle and k_r the wave number in the look direction.

Following H&H the relation between the SAR and RAR images in the pure velocity bunching model is obtained by mapping each facet at position $\mathbf{x}'$ into its corresponding position $\mathbf{x} = \mathbf{x}' + \xi(\mathbf{x}')$ in the image plane, i.e.

$$I_S(\mathbf{x}) = \int_{-\infty}^{\infty} \mathrm{d}\mathbf{x}'\, I_R(\mathbf{x}')\,\delta[\mathbf{x} - \mathbf{x}' - \xi(\mathbf{x}')] \tag{10}$$

The integration over $\mathbf{x}'$ can be readily performed and the result for the SAR image intensity becomes

$$I_S(\mathbf{x}) = \frac{I_R(\mathbf{x}')}{|1 + d\xi(\mathbf{x}')/d\mathbf{x}'|},\ \text{at}\ \mathbf{x}' = \mathbf{x} - \xi(\mathbf{x}') \tag{11}$$

For the case when

$$|d\xi(\mathbf{x}')/d\mathbf{x}'| << 1 \tag{12}$$

a linear relation between the SAR image and the surface elevation amplitude can be established. The inequality, however, only holds for pure swell cases and in general Eq. (10) represents a strongly nonlinear transformation.

3 A general relationship between SAR image spectrum and cumulants of the surface field.

Except for the strongly nonlinear velocity bunching effect, the SAR measurement theory has so far been based on linear arguments. Here we would like to obtain a slightly more general result by allowing weakly nonlinear effects in the surface wave field, and the task is to obtain a closed nonlinear mapping relation between SAR image spectrum and the surface gravity wave spectrum. In order to achieve this we first would like to establish a general relationship between the SAR image and the relevant cumulants of the wave field. This will be done for arbitrary RAR images I_R and azimuthal displacement fields ξ, i.e. we do not need the assumption that these fields are linearly related to the surface elevation. The starting point is Eq. (10) which is a general relation between on the one hand the SAR image intensity and on the other hand the RAR image intensity and the azimuthal displacement.

Introduce the Fourier transform of the SAR image $I_S(\mathbf{x})$,

$$\hat{I}_S(\mathbf{k}) = \frac{1}{(2\pi)^2} \int_{-\infty}^{\infty} \mathrm{d}\mathbf{x}\, I_S(\mathbf{x}) \exp(-i\mathbf{k}.\mathbf{x}). \tag{13}$$

Using Eq. (10) and performing the integration over $\mathbf{x}$ this becomes

$$\hat{I}_S(\mathbf{k}) = \frac{1}{(2\pi)^2} \int_{-\infty}^{\infty} \mathrm{d}\mathbf{x}'\, I_R(\mathbf{x}') \exp(-i\mathbf{k}.(\mathbf{x}' + \xi(\mathbf{x}'))). \tag{14}$$

The SAR image spectrum now follows from the second moment $\langle \hat{I}_S(\mathbf{k}_1)\hat{I}_S^*(\mathbf{k}_2)\rangle$. Using Eq. (14) and some rearrangement gives

$$\langle \hat{I}_S(\mathbf{k}_1)\hat{I}_S^*(\mathbf{k}_2)\rangle = \frac{1}{(2\pi)^4} \int_{-\infty}^{\infty} \mathrm{d}\mathbf{x}_1 \mathrm{d}\mathbf{x}_2\ \exp(-i\mathbf{k}_1.\mathbf{x}_1 + i\mathbf{k}_2.\mathbf{x}_2)\ G(\mathbf{x}_1, \mathbf{x}_2) \tag{15}$$

where

$$G(\mathbf{x}_1, \mathbf{x}_2) = \langle I_R(\mathbf{x}_1) I_R(\mathbf{x}_2) \exp[-i(\mathbf{k}_1.\xi_1 - \mathbf{k}_2.\xi_2)]\rangle. \tag{16}$$

In the next step we utilize the assumption of homogeneity of the ensemble of waves, i.e. we assume that the correlation function $G(\mathbf{x}_1,\mathbf{x}_2)$ is only a function of the difference $\mathbf{r}=\mathbf{x}_1-\mathbf{x}_2$ and not of the mean location $\mathbf{s}=\mathbf{x}_1+\mathbf{x}_2$. To that end we transform in the integral in Eq. (15) the integration variables from the pair $\mathbf{x}_1,\mathbf{x}_2$ to the pair $\mathbf{r},\mathbf{s}$ and because of homogeneity the integration over $\mathbf{s}$ can be performed. The result is

$$\langle \hat{I}_S(\mathbf{k}_1)\hat{I}_S^*(\mathbf{k}_2)\rangle = \frac{1}{4\pi^2}\delta(\mathbf{k}_1-\mathbf{k}_2)\int_{-\infty}^{\infty} \mathrm{d}\mathbf{r}\ \exp(-i\mathbf{k}_1.\mathbf{r})\ G(\mathbf{r}) \tag{17}$$

where

$$G(\mathbf{r}) = \langle I_R(\mathbf{x}+\mathbf{r})I_R(\mathbf{x})\exp\left[-i\mathbf{k}.\left(\xi(\mathbf{x}+\mathbf{r})-\xi(\mathbf{x})\right)\right]\rangle. \tag{18}$$

for arbitrary $\mathbf{x}$. Therefore, the SAR image field is homogeneous as well, and upon introduction of the SAR image spectrum

$$\langle \hat{I}_S(\mathbf{k}_1)\hat{I}_S^*(\mathbf{k}_2)\rangle = F_{SAR}(\mathbf{k}_1)\delta(\mathbf{k}_1-\mathbf{k}_2) \tag{19}$$

one finds the desired result

$$F_{SAR}(\mathbf{k}) = \frac{1}{4\pi^2}\int_{-\infty}^{\infty} \mathrm{d}\mathbf{r}\ \exp(-i\mathbf{k}.\mathbf{r})\ G(\mathbf{r}) \tag{20}$$

The next important step is the evaluation of the ensemble average appearing in the expression of the spatial correlation function $G(\mathbf{r})$. It is evident that the ensemble average involves three stochastic variables, namely $I_R(\mathbf{x}+\mathbf{r})$, $I_R(\mathbf{x})$ and the difference in azimuthal displacement $\Delta\xi=\xi(\mathbf{x}+\mathbf{r})-\xi(\mathbf{x})$, and therefore the ensemble average can only be evaluated when the relevant cumulants, such as mean, standard deviation, skewness, kurtosis, etc. are known. This will be assumed for the moment.

In order to make things slightly easier we now introduce explicitely the fluctuations δI around the mean intensity I_0, or,

$$I = I_0\left(1+\delta I\right),\ \langle \delta I\rangle = 0 \tag{21}$$

and we drop the notation δI in favour of I. Because of homogeneity it is allowed to evaluate the spatial correlation function at the arbitrary location $\mathbf{x}=0$. Then G becomes

$$G(\mathbf{r}) = I_0^2\langle(1+I_R(\mathbf{r}))(1+I_R(0))\exp\left(-i\mathbf{k}.\Delta\xi\right)\rangle, \tag{22}$$

where $\Delta\xi=\xi(\mathbf{r})-\xi(0)$. Krogstad (1992) now made the important remark that ensemble averages of this type may be evaluated by means of the characteristic function of the stochastic process $\mathbf{X}=[I_R(\mathbf{r}),I_R(0),\Delta\xi]$. Here, the characteristic function of $\mathbf{X}$ is defined as

$$K(\mu) = \langle e^{i\mu.\mathbf{X}}\rangle. \tag{23}$$

and μ are auxiliary variables. Note that the characteristic function is nothing but the Fourier transform of the pdf $p(\mathbf{X})$ as

$$\langle e^{i\mu.\mathbf{X}}\rangle = \int \mathrm{d}\mathbf{X}\ p(\mathbf{X})e^{i\mu.\mathbf{X}}. \tag{24}$$

It is now straightforward to show that G of Eq. (22) may be given in terms of $K(\mu)$ and its first and second derivatives at the location $\mu_0=(0,0,-k)$. One has

$$G = I_0^2\left\{K(\mu_0) - i\frac{\partial K}{\partial\mu_1} - i\frac{\partial K}{\partial\mu_2} - \frac{\partial^2 K}{\partial\mu_1\partial\mu_2}\right\},\ \text{at}\ \mu=\mu_0. \tag{25}$$

For a Gaussian sea state the evaluation of G now becomes an almost trivial algebraic task because the characteristic function (which is the Fourier transform of the pdf) is a Gaussian. With B_{ij} the covariance matrix with elements $\langle X_i X_j \rangle$ the characteristic function for the stochastic process $\mathbf{X}$ with zero mean $\langle \mathbf{X} \rangle$ becomes

$$K(\mu) = e^{-\frac{1}{2}\mu_i \mu_j B_{ij}} \tag{26}$$

Krogstad (1991) used Eq. (26) in evaluating G from (25) and he found identical results as H&H for the expression for the SAR image spectrum.[1] It is noted here that this simple algebraic approach can also be extended to fairly general forms of the pdf. A general expression of the pdf of any process $\mathbf{X}$ can, following Gram and Charlier, be given in terms of the cumulants of the stochastic process. The corresponding characteristic function becomes

$$K(\mu) = e^{-\frac{1}{2}\mu_i \mu_j B_{ij}} \left\{ 1 - \frac{i}{3!} \mu_i \mu_j \mu_k C_{ijk} + \frac{1}{4!} \mu_i \mu_j \mu_k \mu_l D_{ijkl} + ... \right\}, \tag{27}$$

where we used the summation convention over repeated indices. Up to fifth order in μ the expansion coefficients are identical to cumulants of the distribution function.

In order to explain the validity of the above expansion we discuss a one dimensional example. According to Cramér (1946) any pdf $p(x)$ of compact support can be expanded in terms of orthogonal functions $f^{(n)}(x) = (d/dx)^n f$ where f is given by the normal distribution $f(x) = \exp(-1/2\, x^2)/(2\pi)^{1/2}$,

$$p(x) = \sum_{n=0}^{\infty} \frac{(-1)^n}{n!} c_n f^{(n)}(x). \tag{28}$$

Here the expansion coefficients can be expressed in terms of the central moments m_n of the pdf $p(x)$. Thus, one finds with zero mean and unit standard deviation that $c_0 = 1$, $c_1 = c_2 = 0$, $c_3 = m_3$, $c_4 = m_4 - 3$, $c_5 = m_5 - 10m_3$, $c_6 = m_6 - 15m_4 + 30$, etc. Alternatively, the expansion coefficients may be expressed in terms of the cumulants κ_n, which are the expansion coefficients when the logarithm of the characteristic function of the pdf is written as a series in μ. One finds $c_3 = \kappa_3$, $c_4 = \kappa_4$, $c_5 = \kappa_5$, $c_6 = \kappa_6 + 10\kappa_3^2$. Thus, the first five expansion coefficients correspond to the cumulants of the distribution function, but not the sixth! As the characteristic function of $p(x)$ is its Fourier transform (see (24)) the n^{th} derivative of $f(x)$ corresponds in the expansion of the characteristic function to a term proportional to $(-i\mu)^n$. Eq. (27) is then just the extension for many stochastic variables.

Let us now determine the general expression for the SAR image spectrum in terms of moments/cumulants of the wave field. To that end we substitute Eq. (27) into Eq. (25) to obtain after some straightforward algebra

$$\begin{aligned} G(\mathbf{r}) = I_0^2 e^{-\frac{1}{2}k^2 B_{33}} \times & \\ \Bigg\{ & \left(1 + \frac{ik^3}{3!} C_{333} + \frac{k^4}{4!} D_{3333}\right) \left(1 + B_{12} - ik(B_{13} + B_{23}) - k^2 B_{13} B_{23}\right) \\ & -ikC_{123} - \frac{k^2}{2!} \left(C_{133} + C_{233} + D_{1233}\right) \\ & + ik^3 \left[\frac{1}{3!} \left(D_{1333} + D_{2333}\right) + \frac{1}{2!} \left(B_{23} C_{133} + B_{13} C_{233}\right) \right] \\ & + \frac{k^4}{3!} \left(B_{23} D_{1333} + B_{13} D_{2333}\right) \Bigg\} \end{aligned} \tag{29}$$

[1] Details are, however, different. Krogstad uses a four dimensional stochastic vector $\mathbf{X} = \left[I_R(\mathbf{r}), I_R(0), \xi(\mathbf{r}), \xi(0)\right]$, but this is not really needed as there are only three different stochastic variables in the problem.

In deriving (29) we have utilized symmetries such as $C_{123} = C_{132}$ etc. This general relationship between the spatial correlation function $G(\mathbf{r})$ and the moments of the wave field is far too complicated to be of practical use. Before we introduce simplifications based on the properties of weakly nonlinear wave fields we mention that the H&H result for the nonlinear mapping relation can be easily obtained by ignoring all the moments except the second order one. As a consequence one finds

$$G(\mathbf{r}) = I_0^2 e^{-\frac{1}{2}k^2 B_{33}} \left(1 + B_{12} - ik(B_{13} + B_{23}) - k^2 B_{13} B_{23}\right) \quad (30)$$

which is in the present context an extremely simple result. Using relations such as

$$\begin{aligned} B_{12} = \langle I_R(\mathbf{r}) I_R(\mathbf{0})\rangle, B_{13} = \langle I_R(\mathbf{r})\Delta\xi\rangle \\ B_{23} = \langle I_R(\mathbf{0})\Delta\xi\rangle, B_{33} = \langle(\Delta\xi)^2\rangle \end{aligned} \quad (31)$$

the exact correspondence with the original H&H result can then readily be established (making use of the linear MTF's of the previous Section). The question now is whether and which of the additional terms in the general relation (29) need to be retained in the mapping relation of the SAR image spectrum. This will be discussed in more detail in the next section.

4 A simplified nonlinear mapping relation for SAR image spectra

In order to simplify the expression for the SAR image spectrum we will make the assumption of weakly non-linear ocean wave fields, which will furnish an estimate of the size of the expansion coefficients in Eq. (29) and which allows to show that indeed one may get a closed expression. The same approach has been followed in the derivation of the rate of change of the spectrum due to nonlinear four-wave interactions.

Weakly nonlinear waves have a wave steepness, defined here as $\varepsilon = k_0 \langle \eta^2 \rangle^{1/2}$ (with k_0 a 'typical' wave number) which is small. The rate of change of the spectrum due to four-wave interactions is then obtained by assuming that the sea state is close to the Normal distribution. Deviations from normality are expressed in terms of the cumulants of the distribution, and for weakly nonlinear waves a consistent ordering of the cumulants κ_n is

$$\kappa_n = \mathcal{O}(\varepsilon^{2n-2}),$$

reflecting the condition that the sea state is close to a Gaussian as the higher-order cumulants κ_n with $n \geq 3$ are relatively small compared to the second order one. However, in the present problem there is an additional parameter which plays an important role, namely $\omega_0\beta$, as this measures the amount of degradation in azimuth resolution owing to the velocity bunching effect. Typically, $\omega_0\beta$ is large, and to get definite answers it is important to assess the relative importance of these two dimensionless parameters.

The size of the parameter [2] β compared to ε is now obtained from the H&H result (30). Apart from the Gaussian factor, the H&H result contains three terms. Their respective sizes are

$$B_{12} = \mathcal{O}(\varepsilon^2),\ B_{13} \simeq B_{23} = \mathcal{O}(\beta\varepsilon^2),\ B_{33} = \mathcal{O}(\beta^2\varepsilon^2) \quad (32)$$

Because there are three terms there are three possibilities to estimate β. Balancing the first and the second term gives $\beta = \mathcal{O}(1)$, while balancing the first and the third, nonlinear term gives $\beta = \mathcal{O}(1/\varepsilon)$. Finally, the balance of the third and second term gives $\beta = \mathcal{O}(1/\varepsilon^2)$. Now, the choice $\beta = \mathcal{O}(1)$ is unrealistic because with the estimate of B_{33} one sees that the damping by velocity bunching is small, on the other hand the choice $\beta = \mathcal{O}(1/\varepsilon^2)$ gives excessive damping. We are therefore left with the estimate

$$\beta = \mathcal{O}(1/\varepsilon). \quad (33)$$

[2] from now on I will be a bit sloppy because actually $\omega_0\beta$ should be used

This gives a damping by velocity bunching of the order one, which is what one should expect. From now on we will refer to this relation as the *velocity bunching ordering*.

For the higher cumulants now the following ordering will be obtained:

$$\begin{aligned} C_{333} = \mathscr{O}(\beta^3\varepsilon^4) = \mathscr{O}(\varepsilon),\ D_{3333} = \mathscr{O}(\beta^4\varepsilon^6) = \mathscr{O}(\varepsilon^2), \\ C_{123} = \mathscr{O}(\beta\varepsilon^4) = \mathscr{O}(\varepsilon^3),\ C_{133} \simeq C_{233} = \mathscr{O}(\beta^2\varepsilon^4) = \mathscr{O}(\varepsilon^2) \\ D_{1233} = \mathscr{O}(\beta^2\varepsilon^6) = \mathscr{O}(\varepsilon^4),\ D_{1333} = \mathscr{O}(\beta^3\varepsilon^6) = \mathscr{O}(\varepsilon^3) \end{aligned} \tag{34}$$

Applying the above ordering to Eq. (29), and retaining only those terms which have a size of $\mathscr{O}(\varepsilon^2)$ or larger we obtain the much simpler expression

$$G(\mathbf{r}) = I_0^2 G_{VB}\left\{1 + B_{12} - ik\left(B_{13} + B_{23}\right) - k^2 B_{13}B_{23} - \frac{k^2}{2!}\left(C_{133} + C_{233}\right)\right\}, \tag{35}$$

where

$$G_{VB}(\mathbf{r}) = e^{-\frac{1}{2}k^2 B_{33}}\left(1 + \frac{ik^3}{3!}C_{333} + \frac{k^4}{4!}D_{3333} - 10\frac{k^6}{6!}C_{333}^2\right). \tag{36}$$

Here, the function G_{VB} is related to the sole effects of velocity bunching as it only involves moments of the azimuthal displacement ξ. It is given by the average of $\langle \exp(-i\mathbf{k}.\Delta\xi)\rangle$ and the presence of the term proportional to C_{333}^2 will be explained in a moment. The other terms in Eq. (35) are the usual terms from the H&H approach, except the term involving the skewness C.

For completeness, we mention that in terms of the moments the relevant expansion coefficients are given by

$$\begin{aligned} C_{333} = \langle(\Delta\xi)^3\rangle,\ D_{3333} = \langle(\Delta\xi)^4\rangle - 3\langle(\Delta\xi)^2\rangle^2 \\ C_{133} = \langle I_R(\mathbf{r})(\Delta\xi)^2\rangle,\ C_{233} = \langle I_R(\mathbf{0})(\Delta\xi)^2\rangle. \end{aligned} \tag{37}$$

The actual determination of the additional expansion coefficients of (37)) in terms of the surface wave spectrum still needs some work. In the context of the linear MTF's of section 2 this is expected to be a straighforward, but laborious task. For example, Janssen (2003) obtained a theoretical expression for the fourth cumulant of the surface elevation by solving in an approximate fashion the Zakharov equation. It is expected that the third cumulants can be expressed in terms of the wave spectrum as well.

The unexpected result is that higher order statistics are *always* required to give an accurate representation of the SAR image spectrum. In the first instance, it was expected that in cases of extreme sea states, such as freak waves are, which may have large deviations from Normal statistics, effects of skewness or kurtosis would be important. However, now it appears that according to Eq. (35) these effects are always relevant. The reason for this is that a SAR flying on board of a polar orbiter always suffers from serious effects of velocity bunching. This is reflected by the large values of β in the velocity bunching ordering. For this reason H&H needed to retain the nonlinear term $B_{13}B_{23}$ in their nonlinear mapping relation. However, to be consistent one needs to retain the skewness terms C_{133} and C_{233} as well. Also, the skewness term C_{333} and the kurtosis term D_{3333} need to be included.

Finally, the question whether there is convergence is of importance. If the nth expansion coefficient c_n of the pdf was just given by the nth cumulant κ_n then the answer would be a straightforward 'yes'. However, as pointed out in section 3, already the sixth-order expansion coefficient c_6 starts to deviate from this regular pattern, as $c_6 = \kappa_6 + 10\kappa_3^3$. Let us consider the velocity bunching term $\langle \exp(-i\mathbf{k}.\Delta\xi)\rangle$ in detail because all the moments in its expansion depend on the azimuthal displacement $\xi = \beta v$ which is formally of $\mathscr{O}(1)$ according to the velocity bunching ordering. The velocity bunching term is equal to the characteristic function $K(\mu)$ of Eq.

(27) where the stochastic process vector $\mathbf{X} = \Delta\xi$ just contains one element. Again, using the velocity bunching ordering it is then straightforward to show that the fifth order expansion coefficient can be neglected because it gives a contribution of $\mathcal{O}(\varepsilon^3)$. However, the sixth-order coefficient gives an $\mathcal{O}(\varepsilon^2)$ contribution, because c_6 is proportional to the square of skewness κ_3, which is of $\mathcal{O}(\varepsilon^2)$ and is much larger than the sixth cumulant $(= \mathcal{O}(\varepsilon^4))$. For this reason we have included the term proportional to C_{333}^2 in the expression for G_{VB} of Eq. (36). Therefore, to be sure, the size of the seventh and eighth-order expansion coefficients was checked as well. These turned out to give contributions that are $\mathcal{O}(\varepsilon^3)$ or smaller and therefore up to $\mathcal{O}(\varepsilon^2)$ Eq. (35) can be regarded as a closed form.

Let us return now to the issue of extreme sea state detection. It was pointed out that it would be desirable to be able to measure quantities such as the skewness of the surface elevation. Here, it is pointed out that an azimuthal cutoff analysis (see, e.g. Kerbaol *et al.*, 1998) might give information on the kurtosis of the pdf of the vertical component of the orbital motion. In order to see this, consider the velocity bunching factor of Eq. (36) and suppose one manages to measure its magnitude. To the required approximation one then obtains

$$|G_{VB}(\mathbf{r})| = e^{-\frac{1}{2}k^2 B_{33}} \left| 1 + \frac{k^4}{4!} D_{3333} \right|, \tag{38}$$

in other words the contribution by the skewness term C_{333} vanishes and all that is left are effects of kurtosis.

5 Conclusions

Recent observations of freak waves and theoretical developments on nonlinear focussing have increased our understanding of the generation of freak waves. A nonlinear, coherent sea state, having a large kurtosis, is most likely to produce these extreme events. This notion is supported by evidence from laboratory studies, however, validation of all this in the field is still required.

It would be most desirable to be able to monitor the kurtosis of the sea surface by means of satellite observations. In theory, the wave form as observed from an altimeter could provide this information (Lipa and Barrick, 1981). In this note we have explored the possibility whether the SAR would be able to give information on the kurtosis of the pdf and hence on extreme sea states.

Extending the approach of H&H by allowing for deviations from Normality and using the method developed by Krogstad (1992) we have obtained a closed form for the SAR image spectrum in terms of cumulants of the ocean wave field. According to the velocity bunching ordering, we find the surprising result that effects of skewness and kurtosis need to be included in the expression for the SAR image spectrum. This is evident when it is realized that velocity bunching is a strongly nonlinear process. In fact, because $\beta = R/V$ is large, details of the sea surface elevation such as skewness and kurtosis are amplified by the SAR imaging process. Therefore, the H&H expression for the SAR image spectrum is not complete, but since the SAR imaging acts like a magnifying glass there may be, at least in theory, a unique opportunity to observe relatively subtle parameters such as skewness and kurtosis.

A Velocity bunching

Consider a SAR on board of a satellite flying at a speed V at a height of about 800 km. The SAR is looking under an incidence angle of about 20° towards the ocean surface and has a finite aperture angle $\Delta\theta$. See for an explanation of some of the details Fig. 2. Suppose that at a certain instant in time the Radar spots an object. Viewed from the SAR the object will be advancing with a speed V along the flight direction and when the object is not in the centre of the aperture cone, it will have a component of the velocity in the direction from which the electro-magnetic waves are propagating. When these waves “reflect” from the object they will have a Doppler shift in the frequency. The location of the object can now be determined very accurately by measuring the Doppler shift while the object is passing, and when the Doppler shift vanishes the object is at the centre of the aperture cone.

However, when the object has itself an ’unknown’ velocity v, because it is sitting on a wavy ocean surface, there will be an additional Doppler shift, which gives rise to a mislocation of the object. Although the ratio v/V is small the azimuthal shift is surprisingly large. Let us calculate the azimuthal shift. The distance between

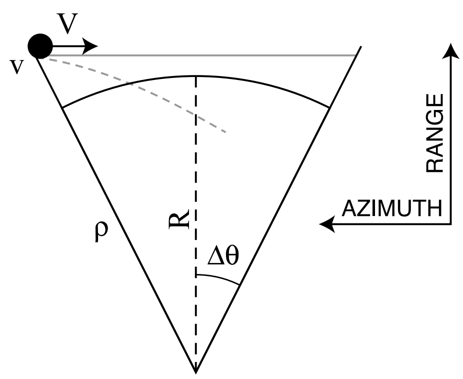

Figure 2: Definition sketch of the velocity bunching problem with a SAR.

the SAR and the object is given by two contributions, namely $\rho_1 = R/\cos\theta$ and $\rho_2 = -vt$, where v is taken positive when the object moves towards the SAR, and time t is defined in such a way that it vanishes when the object is at the centre of the cone. Hence,

$$\rho = R/\cos\theta - vt \tag{A1}$$

Of course, time is directly related to the azimuth angle θ. With Δt the travel time through the aperture cone, one finds

$$\theta = \frac{V}{R}(t - \Delta t/2) \tag{A2}$$

Eliminating time from the expression for ρ one thus finds

$$\rho = R/\cos\theta - \beta v\theta + const \tag{A3}$$

with $\beta = R/V$. The object is now located by minimizing the distance ρ as function of the azimuth angle θ, which is equivalent to the condition of zero Doppler shift. Thus,

$$\frac{\partial\rho}{\partial\theta} = \rho\left[\frac{\sin\theta}{\cos^2\theta} - \frac{v}{V}\right] = 0 \tag{A4}$$

gives the azimuth location of the object. Solving for $\sin\theta$ gives

$$\sin\theta = \frac{-1+\sqrt{1+4(v/V)^2}}{2v/V} \simeq \frac{v}{V} + \mathcal{O}\left(\frac{v}{V}\right)^3 \tag{A5}$$

Since, in practice $v/V \simeq 10^{-4}$ is extremely small, the cubic term may be disregarded and to a very good approximation one finds the azimuthal mismatch $\delta\theta = v/V$. However, in order to obtain the mismatch in azimuthal location ξ one needs to multiply $\delta\theta$ with the range R, which is a large number. Hence

$$\xi = \beta v \tag{A6}$$

For SAR's flying on board of ERS and ENVISAT $\beta = \mathcal{O}(100)$ and since v is $\mathcal{O}(1)$ the azimuthal displacement may easily be of the order of 100 m, i.e. comparable to the wavelength of the dominant surface gravity waves.

References

Alpers, W. and K. Hasselmann, 1978. The two-frequency microwave technique for measuring ocean-wave spectra from airplane or satellite. *Boundary Layer Meteorol.*, **13**, 215-230.

Alpers, W., D.B. Ross and C.L. Rufenach, 1981. On the detectability of ocean surface waves by real and synthetic aperture radar. *J. Geophys. Res.*, **86**, 6481-6498.

Brüning, C., W. Alpers, L.F. Zambresky and D.G. Tilley, 1988: Validation of a SAR ocean wave imaging theory by the shuttle imaging radar-B experiment over the North Sea. *J. Geophys. Res.*, **93**, 15403-15425.

Cramér, H., 1946. *Mathematical Methods of Statistics*, Princeton University Press, Princeton, 575 pp.

Feindt, F.J., J. Schröter and W. Alpers, 1986: Measurement of the ocean wave-radar modulation transfer function at 35 GHz from a sea based platform in the North Sea.*J. Geophys. Res.*, **91**, 9701-9708.

Hasselmann, K, and S. Hasselmann, 1991. On the nonlinear mapping of an ocean wave spectrum into a SAR image spectrum and its inversion. *J. Geophys. Res.*, **C96**, 10713-10729.

Janssen, P.A.E.M., 2003. Nonlinear Four-Wave Interactions and Freak Waves. *J. Phys. Oceanogr.* **33**, 863-884.

Kerbaol, V., B. Chapron, and P.W. Vachon, 1998. Analysis of ERS-1/2 synthetic aperture radar wave mode imagettes. *J. Geophys. Res.*, **C103**, 7833-7846.

Komen, G.J., L. Cavaleri, M. Donelan, K. Hasselmann, S. Hasselmann, and P.A.E.M. Janssen, 1994: *Dynamics and Modelling of Ocean waves* (Cambridge University Press, Cambridge)

Krogstad, H.E., 1992. A simple derivation of Hasselmann's nonlinear ocean-sar transformation. *J. Geophys. Res.*, **C97**, 2421-2425.

Lipa, B., and D.E. Barrick, 1981. Ocean surface height-slope probability density function from SEASAT altimeter echo. *J. Geophys. Res.*, **86**, 10921-10930.

Mori N. and P.A.E.M. Janssen, 2006: On Kurtosis and Occurrence Probability of Freak Waves. *J. Phys. Oceanogr.*, **36**, 1471-1482.

Wright, J.W., 1968: A new model for sea clutter. *IEEE Transactions on Antennas and Propagation*, **AP-16**, 217-223.